Impulsive parametric damping in energy harvesting

Maryam Ghandchi Tehrani[1*] and Thomas Pumhoessel[2]

[1]Institute of Sound and Vibration Research, University of Southampton,
SO17 1EN, Southampton, UK
[2]Institute of Mechatronic Design and Production, Johannes Kepler University
Linz, 4040 Linz, Austria

Abstract. In this paper, an electro-mechanical system with a time-varying damper, which is capable of changing the damping coefficient impulsively, is considered. The effect of the impulsive parametric damping to the modal energy content of the mechanical system is investigated analytically as well as numerically. First, the governing differential equation is presented and then the solution of the system's response is obtained through numerical integration. The energy dissipated by the damper is then calculated to investigate the amount of the energy that can be harvested, and the results are compared with the results from a system without parametric impulses. It is shown, that the amount of the harvested energy can be increased by introducing parametric impulses. Then, an analytical formulation is derived for the system using Dirac-Delta impulses and the analytical results are validated with numerical simulations. The device is subjected to an initial condition and therefore is vibrating freely without any base excitation. This could be used for applications such as harvesting energy from the passage of a train, where the train vibration can introduce an initial velocity to the harvester and the energy can then be extracted from the free vibration of the harvester.

1. Introduction

Parametrically excited systems exhibit interesting dynamic behaviour and have been investigated extensively in the past [1, 2]. Parametric excitation occurs when a parameter of the system varies with time. For example, in civil engineering in cable-stayed bridges the vibration of the deck can axially excite the cables, which results in variation of the stiffness of the cables [3]. In marine applications, the wave motion can generate parametric roll in ships [4]. A small amplitude of disturbance can trigger parametric instability. Recently, Ghandchi Tehrani et al. [5] has implemented an active vibration control strategy to stabilise such systems using velocity and displacement feedback.
Periodic, parametric stiffness excitation at anti-resonance frequencies, discovered by A. Tondl [6], leads to a coupling of the respective modes of vibration and allows to suppress self-excited vibrations [6].

Journal of Physics: Conference Series **744** (2016) 012081 doi:10.1088/1742-6596/744/1/012081

Due to this interaction between the modes, energy is transferred in a periodic manner from one mode to another [7, 8] and vice versa. This characteristic is of potential interest for energy harvesting since the energy can be transferred to a mode with high amplitude of vibration. An interesting example of a parametrically excited system is a tuning fork gyroscope, in which the energy is transferred from vertical to horizontal motion due to coupling between the modes [9].
Pumhoessel et al. [10], for example, has recently investigated the effect of applying parametric stiffness excitation of impulsive type in a controlled manner. It turned out that an appropriate choice of the impulsive strength exists, which allows to control the amplitude of vibration by transferring energy from a weakly damped mode to a mode with higher damping, resulting in a much faster decrease of vibration amplitudes than without impulsive stiffness excitation. In [11], it was demonstrated that this concept is capable of stabilizing a self-excited system.
Most attention has been paid to systems with stiffness modulation. However, parametric excitation with periodic time-varying damping has also been considered for energy harvesting applications [12, 13]. In this paper, the dynamic response of a system with parametric impulsive damping is investigated. First, the free response of a single degree of freedom mechanical oscillator with an impulsive damping is obtained using the analytical methods proposed by Hsu [14] and Zheng-rong [15]. The analytical results are then compared with the results from numerical simulations. It is demonstrated that parametric damping can significantly reduce the amplitude of vibration. The dissipated energy in the damping is also calculated. Finally, a potential application of impulsive parametric damping is presented for energy harvesting from train vibrations. Numerical simulations are carried out based on measured vibration acceleration data of an Intercity 125 UK train and therewith, the effect of impulsive parametric damping on the harvested energy is discussed.

2. Theoretical development

The equation of motion of a single degree of freedom mechanical system with impulsive parametric damping can be written as,

$$m\ddot{x} + \left(c + c_p \sum_{k=1}^{N} \varepsilon_k \delta\left(t - t_k\right) \right)\dot{x} + kx = 0, \tag{1}$$

where, m and k represent the mass and the stiffness of the system. The system possesses a constant damping c, and a time-varying impulsive part, which is made of a series of N Direct delta functions $\delta(t - t_k)$ having the strength of $c_p \varepsilon_k$. Each Dirac delta function can be seen as the simplest representative of e.g. a rectangular shaped impulse. The scaling factor ε_k allows the impulsive strength to be different for each impulse. A sequence of arbitrary and periodic impulses are shown in Figure 1.

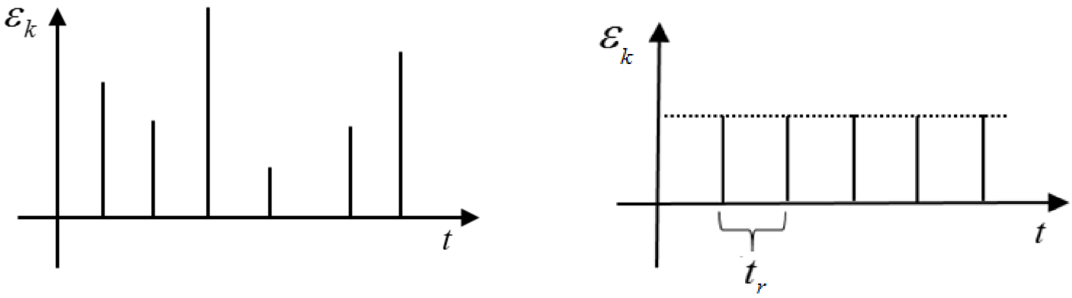

(a) (b)

Figure 1. (a) Arbitrary sequence of impulses (b) periodic sequence of impulses with period t_r

Equation (1) can be rearranged in state-space form such that,

$$\frac{\mathrm{d}}{\mathrm{dt}}\begin{pmatrix} x(t) \\ \dot{x}(t) \end{pmatrix} = \mathbf{G}(t)\begin{pmatrix} x(t) \\ \dot{x}(t) \end{pmatrix} \tag{2}$$

When there is no impulse applied, the mechanical system is of autonomous type, and the response at a time $t = t_0 + t_r$ can be found from the initial time t_0 according to

$$\begin{pmatrix} x(t_0 + t_r) \\ \dot{x}(t_0 + t_r) \end{pmatrix} = \mathbf{I}(t_r) \begin{pmatrix} x(t_0) \\ \dot{x}(t_0) \end{pmatrix} \tag{3}$$

where,

$$\mathbf{I}(t_r) = \mathbf{e}^{\overline{\mathbf{A}} t_r}, \text{ and } \overline{\mathbf{A}} = \begin{bmatrix} 0 & 1 \\ -\dfrac{k}{m} & -\dfrac{c}{m} \end{bmatrix} \tag{4}$$

holds. When an impulse is applied for example at $t = t_k$, the response of the system after the impulse at $t = t_{k+}$ can be obtained from the state-vector of the system just before the impulse at $t = t_{k-}$. Therefore, the delta function is approximated by a rectangular shaped impulse with a fixed total strength but with a duration of the impulse Δt close to zero. Thus, for the interval Δt of an impulse, the response can be obtained from,

$$\begin{pmatrix} x(t_{k+\Delta t}) \\ \dot{x}(t_{k+\Delta t}) \end{pmatrix} = \mathbf{e}^{\mathbf{A}(\Delta t)\Delta t} \begin{pmatrix} x(t_{k^-}) \\ \dot{x}(t_{k^-}) \end{pmatrix} \tag{5}$$

where,

$$\mathbf{A}(\Delta t) = \begin{bmatrix} 0 & 1 \\ -\dfrac{k}{m} & -\dfrac{c}{m} \end{bmatrix} + \begin{bmatrix} 0 & 0 \\ 0 & -\dfrac{\varepsilon_k c_p}{m\Delta t} \end{bmatrix} = \overline{\mathbf{A}} + \mathbf{A}_{p,k}(\Delta t) \tag{6}$$

When $\Delta t \to 0$, then $\overline{\mathbf{A}}\Delta t \to \mathbf{0}$ and $\mathbf{A}_{p,k}$ can be written in the form

$$\mathbf{A}_{p,k} = \begin{bmatrix} 0 & 0 \\ 0 & -\dfrac{\varepsilon_k c_p}{m} \end{bmatrix} \tag{7}$$

Therewith, Eq. (5) reads,

$$\begin{pmatrix} x(t_{k^+}) \\ \dot{x}(t_{k^+}) \end{pmatrix} = \mathbf{e}^{\mathbf{A}_{p,k}} \begin{pmatrix} x(t_{k^-}) \\ \dot{x}(t_{k^-}) \end{pmatrix}, \tag{8}$$

where $\mathbf{J} = \mathbf{e}^{\mathbf{A}_{p,k}}$ is called the jump transfer matrix, similarly to [14], for the kth impulse. in the preceding case, where the matrix $\mathbf{A}_{p,k}$ is given in the form of eq. (7), the matrix exponential $\mathrm{e}^{\mathbf{A}_{p,k}}$ in eq. (8) can be calculated easily. obviously, the jump transfer matrix

$$\mathbf{J} = \begin{bmatrix} 1 & 0 \\ 0 & \mathrm{e}^{-\frac{\varepsilon_k c_p}{m}} \end{bmatrix}. \tag{9}$$

As expected, a damping impulse of Dirac delta form affects only the velocity of the mass m, the displacement remain unchanged, i.e.

$$x(t_{k+}) = x(t_{k-}) \tag{10}$$

and

$$\dot{x}(t_{k+}) = \mathrm{e}^{-\frac{\varepsilon_k c_p}{m}} \dot{x}(t_{k-}) \tag{11}$$

holds. The corresponding variation of the kinetic energy ΔKE_k is given by

$$\Delta KE_k = KE_{k+} - KE_{k-} = \frac{m}{2}(\mathrm{e}^{-2\frac{\varepsilon_k c_p}{m}} - 1)\dot{x}^2(t_{k-}) = (\mathrm{e}^{-2\frac{\varepsilon_k c_p}{m}} - 1)KE_{k-} \tag{12}$$

where KE_{k-} and KE_{k+} represent the kinetic energy just before/after application of the impulse. For an arbitrary sequence of impulses as shown in Figure 1(a),

$$\begin{pmatrix} x(t) \\ \dot{x}(t) \end{pmatrix} = \mathbf{I}(t-t_k)\mathbf{J}_k\mathbf{I}(t_k - t_{k-1})\cdots\mathbf{J}_3\mathbf{I}(t_3-t_2)\mathbf{J}_2\mathbf{I}(t_2-t_1)\mathbf{J}_1\mathbf{I}(t_1)\begin{pmatrix} x(t_0) \\ \dot{x}(t_0) \end{pmatrix} \tag{13}$$

holds. If the sequence of impulses is periodic in time, see Figure 1(b), the response of the system at the end $t_{k+1,+}$ of a period t_r can be obtained from the autonomous system matrix $\mathbf{I}$, the jump transfer matrix $\mathbf{J}$, and the states of the system at the beginning t_{k+} of a period according to

$$\begin{pmatrix} x(t_{k+1,+}) \\ \dot{x}(t_{k+1,+}) \end{pmatrix} = \mathbf{J}_{k+1}\mathbf{I}(t_r)\begin{pmatrix} x(t_{k+}) \\ \dot{x}(t_{k+}) \end{pmatrix} \tag{14}$$

The sum of the kinetic energy and the potential energy can be obtained from,

$$KE + PE = \frac{1}{2}kx^2 + \frac{1}{2}m\dot{x}^2 \tag{15}$$

The energy dissipated in the constant damper can be found from,

$$E_{diss} = c\int_0^t \dot{x}^2 dt \tag{16}$$

The energy extracted by the impulsive damper is,

$$E_{extrs} = \sum_{k=1}^{N} \Delta KE_k = \frac{m}{2}\sum_{k=1}^{N}(\mathrm{e}^{-2\frac{\varepsilon_k c_p}{m}} - 1)\dot{x}^2(t_{k-}) \tag{17}$$

In the next section, some numerical results are presented, underlining the capabilities of impulsive damping in energy harvesting.

3. Numerical Results

A mechanical system with the following parameters is considered:

$$m = 1kg, \quad k = 1N/m, \quad \mathrm{c} = 0.01\mathrm{Ns/m}, \quad \mathrm{c_p} = 1\mathrm{Ns/m},\ \varepsilon{=}0.1,\ \Delta\mathrm{t}{=}0.001\mathrm{s}, \tag{18}$$

The initial conditions are $x(0) = 0, \dot{x}(0) = 1$. The displacement response of the system is obtained analytically from Eq. (13) and is shown in Figure 2(a), see red-dotted line. For the sake of comparison, the response is also obtained from time domain simulation using Matlab ode45. The numerical result (red-solid line) shows a very good agreement with the analytical displacement (dots). The blue-colored lines represent the results of the mechanical system where only natural damping is present. It can be seen that the system with parametric damping can significantly reduce the amplitude of the response. Impulsive damping can therefore be used in active vibration control.

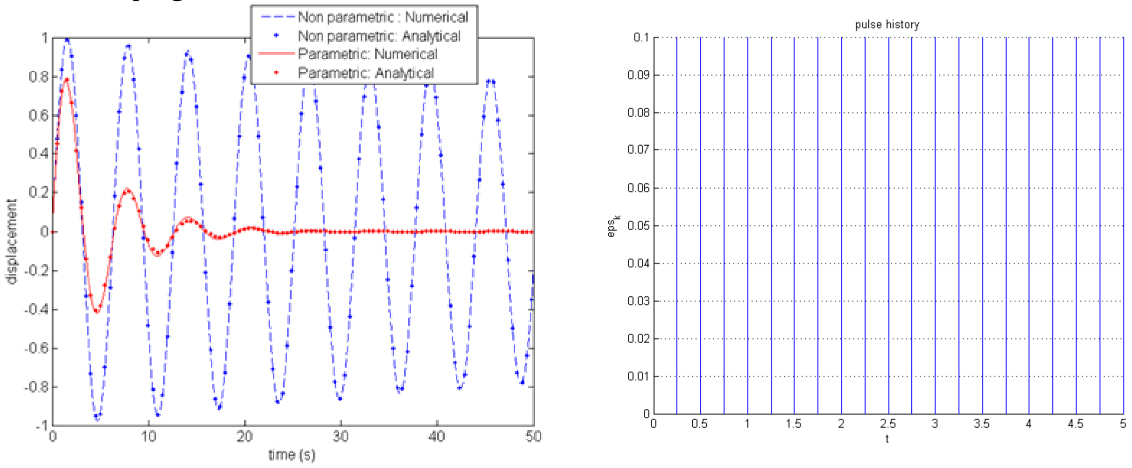

(a) (b)

Figure 2: (a) displacement for parametric (solid line) and nonparametric system (dashed line), and (b) impulsive periodic damping

The sum of the kinetic and the potential energy as well as the dissipated energy are plotted in Figure 3 for both parametric, marked with red solid line, as well as the non-parametric system, marked with blue dashed line. The total energy of the parametric system, is reduced fairly quickly compared to the non parametric system, which underlines the capability of impulsive damping to reduce vibrations of mechanical systems efficiently.

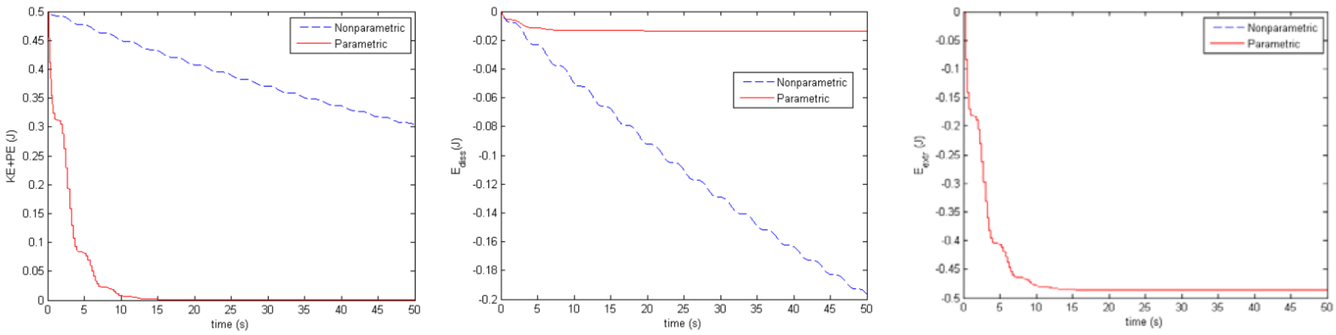

(a) (b) (c)

Figure 3: (a) Kinetic and potential energy for a parametric system (solid line) and a nonparametric system (dashed line), and (b) comparison of dissipated energy, and (c) the extracted energy by impulsive damper

4. Application in energy harvesting from train vibrations

A vibration signal obtained from an Inter-city 125 [16] is used as base excitation of the harvester. The train, which is depicted in Figure 4, consists of 2 diesel power cars, one at each end, with 7 passenger coaches between them. Each vehicle is supported by four wheelsets arranged in two bogies; the bogie wheelbase is 2.6 m in each case. The power cars are 17.8 m long while the trailer vehicles are 22.9 m long. The distance between bogie centres is 16.0 m for the trailer vehicles and 10.3 m for the power cars.

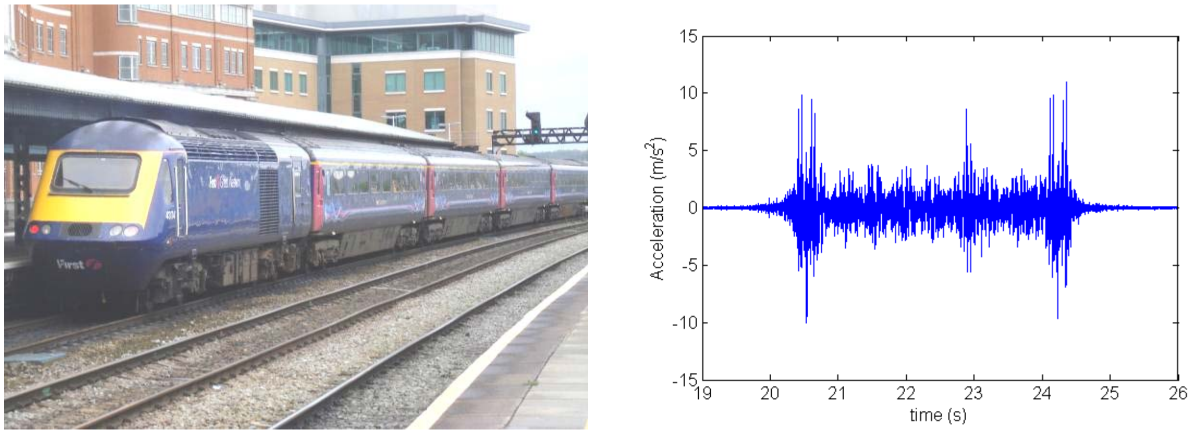

(a) (b)

Figure 4: (a) Photograph of an Inter-city 125 train, and (b) measured acceleration on the sleeper for an Inter-city 125 passing at a speed of 195 km/h.

The measured acceleration of the sleeper during the passage of an Inter-city 125 train at a speed of 195 km/h (54.2 m/s) is shown in Figure 5. The measured acceleration data is integrated to obtain the vertical velocity due to a passing train and is shown in Fig. 5(a). Figure 5(b) depicts the amplitude spectrum of the vertical velocity. In this figure the dominant frequencies, in which the most significant amount of energy can be harvested can be seen. The dominant frequencies, corresponding to the highest peaks are at about 2.4 Hz, 4.8 Hz, 7.1 Hz, 14.3 Hz, 16.6 Hz and 21.3 Hz.

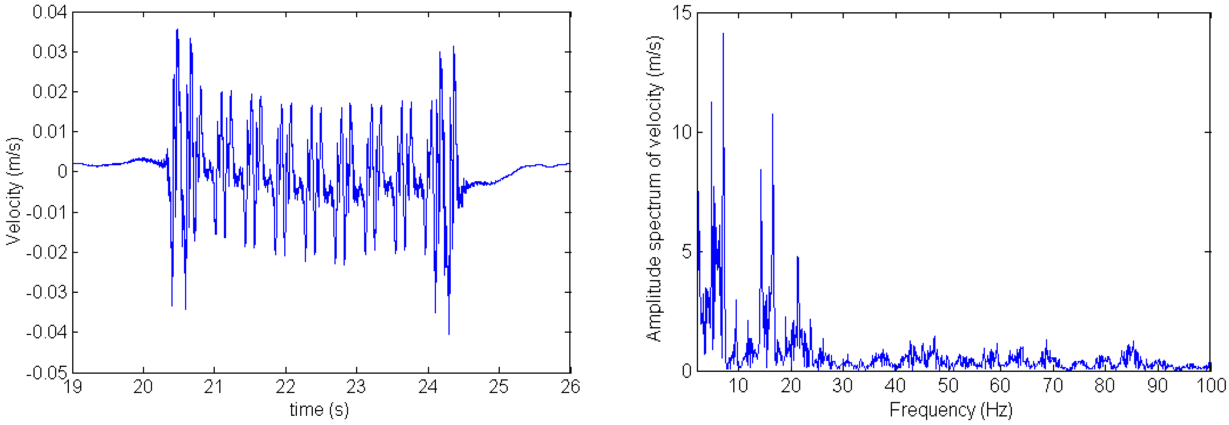

(a) (b)

Figure 5: Velocity data derived from the experimental measurements in Fig. 4(b): (a) time-history and (b) amplitude spectrum.

As discussed above, the acceleration data from the train-induced vibrations is used as the base excitation of an energy harvester with one degree of freedom. By contrast to the mechanical model described in section 2, the sequence of Dirac delta impulses $\sum_{k=1}^{N}\varepsilon_k\delta\left(t-t_k\right)$ is replaced by an equidistant series of rectangular shaped ones according to

Journal of Physics: Conference Series **744** (2016) 012081 doi:10.1088/1742-6596/744/1/012081

$$p(t)=\sum_{k=1}^{N}p_k\left(t\right) \tag{19}$$

where

$$p_k\left(t\right)=\begin{cases} p=\text{const.} & \text{if} \quad t_k\le t\le t_k+\Delta t \\ 0 & \text{otherwise.}\end{cases} \tag{20}$$

The period t_r, pulse-width Δt and amplitude p used for the numerical simulations are given by

$$t_r=0.25, \quad \Delta t=0.0125, \quad p=40. \tag{21}$$

Hence, for the impulsive strength (intensity) $\kappa=c_p\Delta t p=0.5$ holds, where $c_p=1Ns/m$ was used. Figure 6 depicts the sequence of applied rectangular shaped impulses.

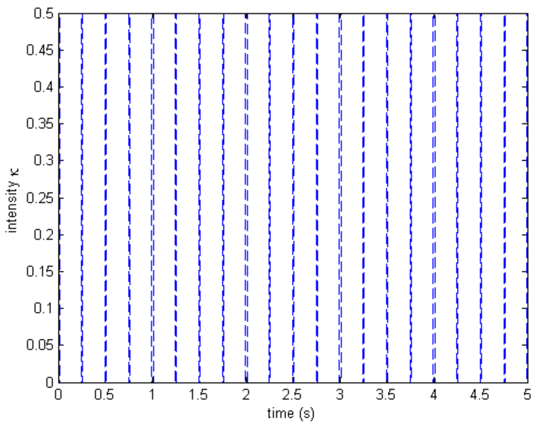

Figure 6: Parametric impulsive damping with the period of $t_r=0.25$, pulse width $\Delta t=0.0125$ and amplitude $p=40$.

The mass m of the harvester is fixed at $m=1kg$, and the stiffness of the harvester is chosen to be $k=1.99\times10^3\,N/m$ so that the natural frequency of the device is 7.1Hz, which corresponds to the dominant frequency in the velocity spectrum in Figure 5(b). Moreover, the constant linear damping coefficient was selected to $c=0.5Ns/m$. A Simulink model was generated to calculate the instantaneous power and the total energy harvested for the passage of a single train at this natural frequency. A Matlab solver (ode15s), with the convergence tolerance of 10^{-6}, and a fixed time step of 1ms was used at every tuning frequency to obtain the displacement, the instantaneous dissipated power, and the total energy extracted from the impulsive parametric damping for the passage of a single train at this natural frequency. The displacement with and without parametric damping is shown in Figure 7(a). As shown previously, the parametric impulsive damping can extract energy from the system. The instantaneous dissipated power in the constant damper and the instantaneous extracted power from the impulsive damper are obtained numerically and plotted in Figure 8 from,

$$P_{diss}=c\dot{x}^2(t), \;\; P_{extr}=c_p\,p(t)\dot{x}^2(t) \tag{22, 23}$$

Journal of Physics: Conference Series **744** (2016) 012081 doi:10.1088/1742-6596/744/1/012081

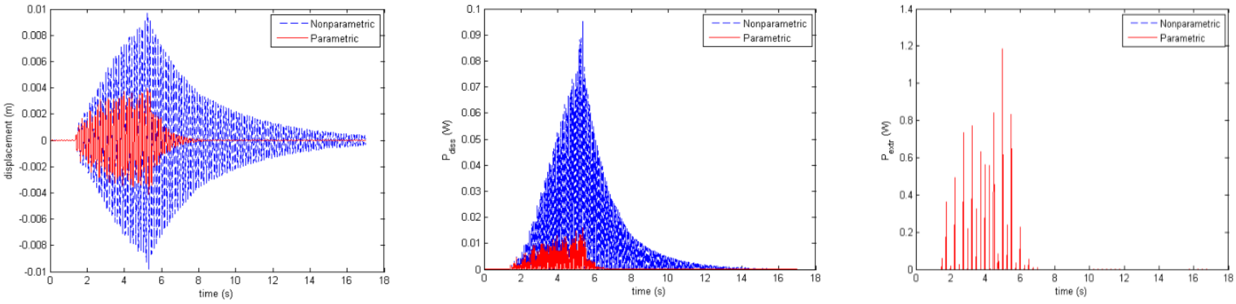

Figure 7: (a) The relative displacement of the harvester (b) the instantaneous dissipated power (c) the instantaneous extracted power with (red solid line) and without (blue dashed line) parametric damping at 7.1Hz

Using the parametric impulsive damping, reduces the instantaneous dissipated power as can be seen in Figure 7(b). The dissipated energy and the extracted energy are calculated from integrating the instantaneous power from 0 to 18s. The impulsive parametric damping reduces the loss of energy by 8 times. The extracted energy is about 0.06J.

Similar analysis has been carried out when the frequency of the harvester is tuned at 16.4Hz see Figure (8). In this case the dissipated energy is reduced by 4.5 times. The extracted energy by the impulsive damper is about 0.1J.

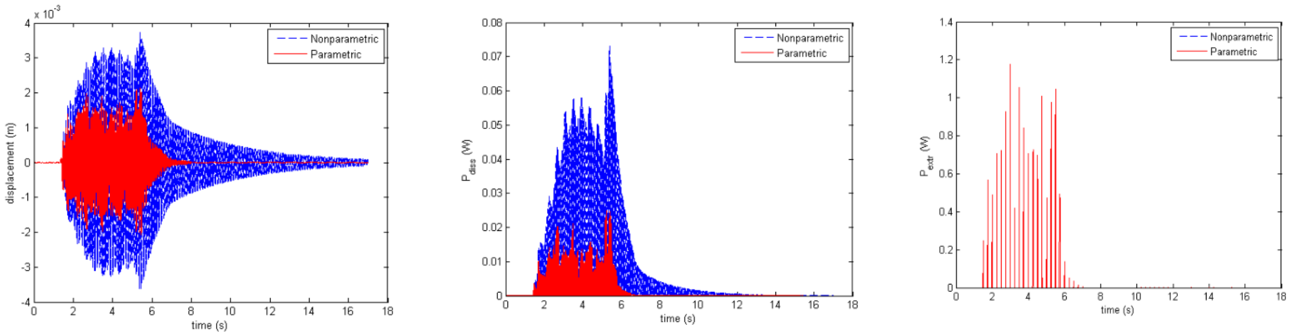

(a) (b) (c)

Figure 8: (a) The relative displacement (b) the instantaneous dissipated power (b) the instantaneous extracted power with (red solid line) and without (blue dashed line) parametric damping at 16.4Hz

The stiffness of the harvester is varied, so that its natural frequency is tuned between 1 and 25 Hz with a step of 0.1429 Hz. The extracted energy was then found by integrating the instantaneous power in the impulsive damper over 18 seconds. Figure 9(a) shows the results. It can be seen that when the harvester is tuned at the dominant frequencies corresponding to about 7.1 Hz, 14.3 Hz, 16.6 Hz and 21.3 Hz, a relatively high amount of energy can be extracted compared to other frequencies. The ratio between the dissipated energy with parametric damping and without parametric damping is also shown in Figure 9(b).

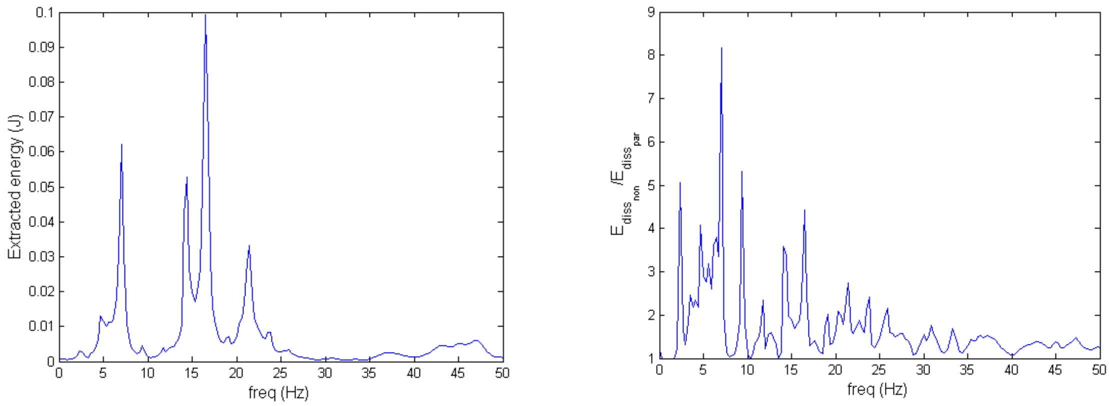

Figure 9: (a) Energy extracted by the impulsive damping as a function of the tuning frequency of the oscillator, (b) ratio between the dissipated energy with and without impulsive damping

The intensity of the impulsive damping, κ, is varied from 0.05 to 10 with a step of 0.05 and the dissipated energy and the harvested energy are plotted for the two frequencies of 7.1Hz and 16.4Hz, see Figure 10 (a) (b). In this range, there is an optimum impulsive damping for each frequency, which maximises the amount of the harvested energy. For example, the optimum intensity is $\kappa = 0.52$ at 7.1Hz, which extracts maximum energy. Larger intensities leads to higher loss of energy.

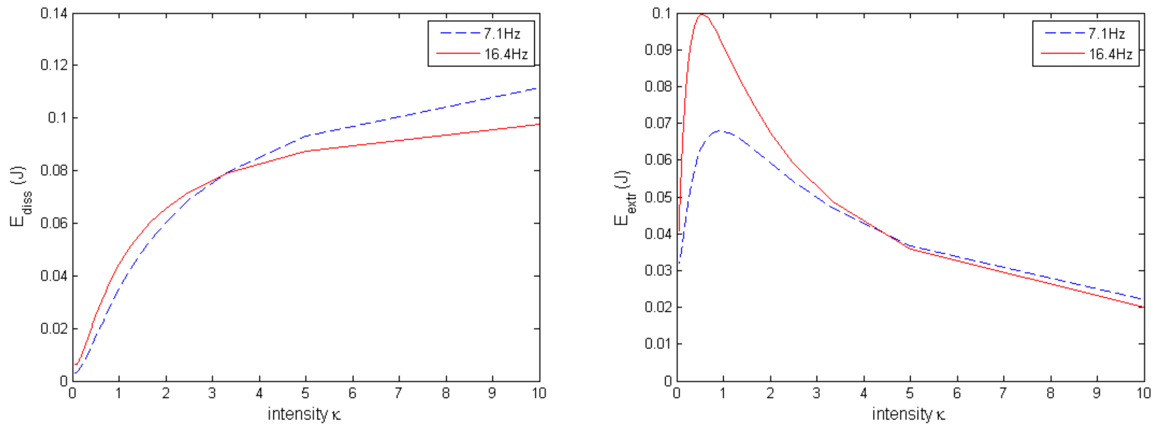

(a) (b)

Figure 10: (a) Dissipated energy and (b) harvested energy versus the intensity of the impulsive damping at the two frequencies of 7.1Hz (blue dashed line) and 16.6Hz (red solid line)

5. Conclusions

In this paper, the dynamic response of a parametrically excited system with impulsive damping is presented. First, the analytical solution is derived and validated with the results from numerical simulation. The displacement of the parametric system is compared with the non-parametric system. It can be seen that impulsive damping can reduce the amplitude of vibration. A potential application of impulsive damping is to harvest energy from train vibrations. Numerical simulation is carried out using the measured acceleration data from the passage of train and the harvested energy are obtained using the parametric impulsive damping for two different frequencies. It is shown that there is an optimum intensity of the impulse, which maximizes the amount of harvested energy.

Acknowledgments
The work of Dr. Thomas Pumhoessel has been supported by the Austrian COMET-K2 programme of the Linz Center of Mechatronics (LCM), and has been funded by the Austrian federal government and the federal state of Upper Austria.

6. References

[1] M. Cartmell, Introduction to Linear, Parametric and Nonlinear Vibrations. London: *Chapman & Hall, 1990.*

[2] A.H. Nayfeh, P.F. Pai, Linear and Nonlinear Structural Mechanics. *Wiley, New York, 2004.*

[3] A. Gonzalez-Buelga, S.A. Neild, D.J. Wagg and J.H.G. Macdonald, Modal stability of inclined cables subjected to vertical support excitation, *Journal of Sound and Vibration, 318, (2008),* 565-579

[4] TM Ahmed, DA Hudson and P Temarel, An investigation into parametric roll resonance in regular waves using a partly non-linear numerical model. *Ocean Engineering 37:2010*, 1307–1320.

[5] M. Ghandchi Tehrani and M. K. Kalkowski, Active control of parametrically excited systems, *Journal of Intelligent Material Systems and Structures, 2015*, 1-13.

[6] A. Tondl, To the problem of quenching self-excited vibrations, *Acta Technica CSAV, 43 (1998)* 109-116.

[7] F. Dohnal, Damping by Parametric Stiffness Excitation: Resonance and Anti-Resonance, *Journal of Vibration and Control 14 (2008)* 669-688.

[8] H. Ecker, T. Pumhoessel, Vibration suppression and energy transfer by parametric excitation in drive systems, *Proc. IMechE PartC: J. Mechanical Engineering Science 226(8) (2012)* 2000-2014.

[9] M. Ghandchi Tehrani, J.M. Balthazar, M. Silveira, Parametric study of a macro-scale tuning fork gyroscope, *ICOEV 2015, Slovenia, 2015*.

[10] T. Pumhoessel, P. Hehenberger and K. Zeman, On the effect of impulsive parametric excitation to the modal energy content of Hamiltonian systems, *ICOVP2013, Lisbon, 9-12 September 2013.*

[11] T. Pumhoessel, A contribution to the reduction of self-excited vibrations of dynamical systems by impulsive parametric excitation, *ICOVP2015, Ljubljana, Slovenia, 7-10 September 2015*.

[12] F. Di Monaco, M. Ghandchi Tehrani, S. J. Elliott, E. Bonisoli, Energy Harvesting using semi-active control, *Journal of Sound and Vibration, 332(23),2013*, 6033-6043.

[13] M. Scapolan, M. Ghandchi Tehrani and E. Bonisoli, Energy harvesting using parametric resonance system due to time-varying damping, *Mechanical Systems and Signal Processing, Accepted October 2015.*

[14] C.S. Hsu, Impulsive Parametric Excitation: Theory, *Journal of Applied Mechanics 39 (1972)* 551-558.

[15] L. Zheng-rong, Discontinuous and impulsive excitation, *Journal of Applied Mathematics and Mechanics, 8(1), 1987*, 31-35.

[16] M. Ghandchi Tehrani, G. Gatti, M.J. Brennan and D.J. Thompson, Energy harvesting from train vibrations, International conference of vibration problems, *ICOVP2013, Lisbon, Portugal, September 2013.*